International Journal of Nanomedicine

Dovepress
open access to scientific and medical research

Open Access Full Text Article

ORIGINAL RESEARCH

Silica Nanoparticles Disturb Ion Channels and Transmembrane Potentials of Cardiomyocytes and Induce Lethal Arrhythmias in Mice

This article was published in the following Dove Press journal:
International Journal of Nanomedicine

Ya-Qin Liu,[1,*] Si-Meng Xue,[1,*] Peng Zhang,[1,*] Lin-Na Xu,[1] De-Ping Wang,[2] Guang Li,[1] Ji-Min Cao[1,2]

[1]Key Laboratory of Medical Electrophysiology of Ministry of Education and Medical Electrophysiological Key Laboratory of Sichuan Province, Institute of Cardiovascular Research, Collaborative Innovation Center for Prevention and Treatment of Cardiovascular Disease of Sichuan Province, Southwest Medical University, Luzhou, Sichuan 646000, People's Republic of China; [2]Key Laboratory of Cellular Physiology at Shanxi Medical University, Ministry of Education, Department of Physiology, Shanxi Medical University, Taiyuan, Shanxi 030001, People's Republic of China

*These authors contributed equally to this work.

Correspondence: Guang Li
Key Laboratory of Medical Electrophysiology of Ministry of Education and Medical Electrophysiological Key Laboratory of Sichuan Province, Institute of Cardiovascular Research, Collaborative Innovation Center for Prevention and Treatment of Cardiovascular Disease of Sichuan Province, Southwest Medical University, 319 Zhongshan Road Section 3, Jiangyang District, Luzhou 646000, Sichuan Province, People's Republic of China
Tel +86 830-3161222
Fax +86 830 3161222
Email liguang@swmu.edu.cn

Ji-Min Cao
Key Laboratory of Cellular Physiology at Shanxi Medical University, Ministry of Education, Department of Physiology, Shanxi Medical University, 56 Xin Jian Nan Lu Road, Taiyuan 030001, Shanxi Province, People's Republic of China
Tel +86 351 4235246
Fax +86 351 4135117
Email caojimin@126.com

Background: The toxicity of silica nanoparticles (SiNPs) on cardiac electrophysiology has seldom been evaluated.

Methods: Patch-clamp was used to investigate the acute effects of SiNP-100 (100 nm) and SiNP-20 (20 nm) on the transmembrane potentials (TMPs) and ion channels in cultured neonatal mouse ventricular myocytes. Calcium mobilization in vitro, cardiomyocyte ROS generation, and LDH leakage after exposure to SiNPs in vitro and in vivo were measured using a microplate reader. Surface electrocardiograms were recorded in adult mice to evaluate the arrhythmogenic effects of SiNPs in vivo. SiNP endocytosis was observed using transmission electron microscopy.

Results: Within 30 min, both SiNPs (10^{-8}–10^{-6} g/mL) did not affect the resting potential and I_{K1} channels. SiNP-100 increased the action potential amplitude (APA) and the I_{Na} current density, but SiNP-20 decreased APA and I_{Na} density. SiNP-100 prolonged the action potential duration (APD) and decreased the I_{to} current density, while SiNP-20 prolonged or shortened the APD, depending on exposure concentrations and increased I_{to} density. Both SiNPs (10^{-6} g/mL) induced calcium mobilization but did not increase ROS and LDH levels and were not endocytosed within 10 min in cardiomyocytes in vitro. In vivo, SiNP-100 (4–10 mg/kg) and SiNP-20 (4–30 mg/kg) did not elevate myocardial ROS but increased LDH levels depending on dose and exposure time. The same higher dose of SiNPs (intravenously injected) induced tachyarrhythmias and lethal bradyarrhythmias within 90 min in adult mice.

Conclusion: SiNPs (i) exert rapid toxic effects on the TMPs of cardiomyocytes in vitro largely owing to their direct interfering effects on the I_{Na} and I_{to} channels and Ca^{2+} homeostasis but not I_{K1} channels and ROS levels, and (ii) induce tachyarrhythmias and lethal bradyarrhythmias in vivo. SiNP-100 is more toxic than SiNP-20 on cardiac electrophysiology, and the toxicity mechanism is likely more complicated in vivo.

Keywords: silica nanoparticle, cardiac electrophysiology, transmembrane potential, ion channel, nanotoxicology

Introduction

Silica (SiO_2) nanoparticles (SiNPs) are becoming one of the most popular materials in many fields because of their unique physical and chemical properties. In the industrial field, SiNPs have been used for organic synthesis, semiconductor production, energy application, and sewage treatment.[1–4] In the biomedical field, SiNPs are applied for food safety inspection, parasite diagnosis, molecular probes, imaging diagnosis, promotion of vascular regeneration, and oncotherapy, etc.[5–12] Synthetic SiNPs can enter the bodies of patients and healthy people through the skin, the respiratory tract, the

digestive tract, and medical exposure, thus raising a biosafety concern about this nanomaterial. Increasing studies indicate that SiNPs can exert biological effects and toxicities after exposure. For example, SiNPs (i) induce systemic toxicity, oxidative stress and DNA damage in the lung, kidney, liver, heart, and brain of mice after intraperitoneal administration for 24 h,[13] (ii) inhibit gap junction communication to promote apoptosis in H9c2 cells via the mitochondrial pathway,[14] (iii) induce pulmonary inflammation, myocardial ischemic damage, and atrio-ventricular conduction block,[15] (iv) cause organ abnormalities during zebrafish embryo development especially the blood vessels and heart,[16,17] (v) inhibit macrophage activity in zebrafish embryos,[18] and (vi) impair cellular ATP supply and reduce the contraction frequency of cardiomyocytes.[19] However, until now, although many studies have focused on the chronic pathological effects of SiNPs, the acute hazardous effects of SiNPs on the heart, especially on cardiac electrophysiology and arrhythmogenesis, have rarely been investigated. Because the heart is one of the most important organs in maintaining life, it is necessary to better understand the toxicities of SiNPs on cardiac electrophysiology.

The heart acts as a pump to maintain blood circulation in the body. Myocardial contraction is generated by the rhythmic excitation-contraction coupling which is initiated by the action potential (AP) from the sinus node. The AP propagates along the conducting system and the working myocardium and then triggers cardiac muscle contraction via the membranous and sarcoplasmic Ca^{2+} signaling. Myocardial AP plays an essential role in the process of heart beating. It is known that the generation and configuration of the AP are decided by the activities of several ion channels, including the inwardly rectifying K^+ (I_{K1}) channel, the voltage-gated Na^+ (I_{Na}) channel, the L-type Ca^{2+} ($I_{Ca\text{-}L}$) channel, the transient outward K^+ (I_{to}) channel, and the delayed rectifying K^+ (I_K) channel.[20,21] Agents such as poisons, drugs, and nanomaterials could do harm to the depolarization and/or repolarization of APs through interfering with the normal activities of these ion channels and thus may cause cardiac dysfunction and arrhythmias if the agent interferes with the normal activities of these ion channels. The objectives of the present study were to examine the potential hazardous effects of SiNPs on several aspects of cardiac electrophysiology, including ion channels, APs, and arrhythmogenesis, and to further explore the underlying mechanisms. The study provides new information and warnings with respect to the utilization of SiNPs in the fields of nanobiology and nanomedicine.

Materials and Methods

Ethical Approval

The animal use protocol was approved by the Ethics Committee of Southwest Medical University for animal experiments (approval No. 201705-093) and followed the ARRIVE guidelines and the US National Institutes of Health Guidelines for the Care and Use of Laboratory Animals (NIH Publication 85-23, revised 1985). Cardiomyocytes used in the study were harvested from the experimental animals.

Preparation and Characterization of SiNPs

SiNPs with particle diameters of 100 nm (SiNP-100) and 20 nm (SiNP-20) were purchased from NanoComposix (San Diego, CA, USA), and were filter-sterilized before use. Both SiNPs were diluted with basal (serum-free) medium or corresponding bath solutions for in vitro studies, or dissolved in 5% isotonic glucose solution for in vivo experiments. Dynamic light scattering (DLS) and electrophoretic light scattering (ELS) techniques were used to characterize the physicochemical properties of SiNPs. Both SiNP-100 and SiNP-20 were dispersed in 1 mL of the corresponding medium or solution for in vitro experiments including in distilled water, basal medium, bath solutions for recording transmembrane potentials (TMPs) and various ion channel currents, and 5% isotonic glucose solution for in vivo experiments. SiNPs were incubated in these media for 5 min at room temperature before use.

Isolation and Culture of Neonatal Mice Ventricular Myocytes

Ventricular myocytes (hereafter referred to as cardiomyocytes) were obtained from neonatal C57BL/6J mice (24–48 h after birth). Mice were sacrificed, hearts were harvested, and ventricular tissues were rapidly cut out and put into pre-cold phosphate buffer solution (PBS) and washed with PBS for several times to remove blood. To isolate cardiomyocytes, ventricular tissues were digested with diluted trypsin solution (0.25% trypsin: PBS = 1:3) at 4°C for overnight (not exceeding 16 h), followed by digestion with type II collagenase (filter-sterilized prior to experiments) for 90 sec at 37°C. The digestion was then stopped with an equal volume of 10% fetal bovine serum (FBS), and the cell suspension was harvested by centrifugation at 800 rpm for 3 min. The supernatant was discarded, and ventricular myocytes were gently resuspended in high-glucose DMEM supplemented with 10% FBS,

penicillin, and streptomycin. Fibroblast growth inhibitor (Brdu) was added at a final concentration of 10 mM to the cell suspension. Cardiomyocytes with good morphology and pulsation were cultured for 24 h and used to perform whole-cell patch-clamp experiments.

Patch-Clamp

A whole-cell configuration of the patch-clamp technique was used to record TMPs and channel currents of cardiomyocytes using the EPC-10 patch-clamp amplifier and PatchMaster software (Heka Elektronik, Lambrecht, Germany) at room temperature (22–25°C). Glass microelectrode pipettes were pulled by a P-97 horizontal puller (Sutter Instruments, Novato, CA, USA). Cells with smooth surfaces and good refractive properties were selected for experiments.

The current clamp mode was used to record TMPs. The bath solution contained (in mM): NaCl 137, KCl 5.4, $MgCl_2$ 1, NaH_2PO_4 0.33, HEPES 10, glucose 10, and $CaCl_2$ 1.8, and pH was adjusted to 7.4 with NaOH. The pipette solution contained (in mM): potassium gluconate 123, NaCl 9, $MgCl_2$ 1.8, HEPES 9, EGTA 0.9, creatine phosphate disodium 14, and Mg-ATP 4, and pH was adjusted to 7.2 with KOH. The acute effects of SiNPs (10^{-8}–10^{-6} g/mL) on the TMPs of cardiomyocytes were recorded within 30 min after exposure and compared with baseline (control).

The voltage-clamp mode was used to record ion channel currents. The I_{K1}, I_{Na} and I_{to} channel currents of cardiomyocytes were recorded at baseline and after exposure to SiNPs for 5–30 min.

To record I_{K1}, the bath solution contained (mM): NaCl 136, $MgCl_2$ 1, KCl 5, HEPES 10, glucose 10, $CaCl_2$ 1.8, and $CdCl_2$ 0.2, and pH was adjusted to 7.4 with NaOH. Pipettes were filled with a solution containing (mM): KCl 150, HEPES 5, EGTA 5, $MgCl_2$ 1, Mg-ATP 1, K_2-ATP 3, and 4-aminopyridine (4-AP) 5, and pH was adjusted to 7.4 with KOH. I_{K1} was elicited by 500-ms depolarizing pulses stepping from −120 mV to +20 mV from a holding potential of −20 mV, with 10 mV increments.

To record I_{Na}, the bath solution contained (in mM): N-methyl-D-glucamine 125, $CaCl_2$ 1, KCl 2.5, $MgCl_2$ 1, NaCl 15, and HEPES 10, and pH was adjusted to 7.4 with HCl. The pipettes solution contained (in mM): NaCl 10, EGTA 10, CsF 105, Na_2-ATP 5, and HEPES 10, and pH was adjusted to 7.3 with CsOH. The steady-state activation of I_{Na} channels was recorded by 50 ms depolarizing pulses from −90 mV to +20 mV from a holding potential of –90 mV, with 10-mV increments. The inactivation kinetics of I_{Na} channels were measured with a double-pulse protocol: the 100-ms serial conditioning pre-pulses in 5-mV steps were applied at a holding potential of –90 mV to achieve serial membrane potentials from −140 mV to −20 mV. A 20-ms testing pulse was delivered at each membrane potential to check the inactivation state of the channels.

To record I_{to}, the bath solution contained (in mM): NaCl 135, $MgCl_2$ 1, KCl 5.4, HEPES 10, NaH_2PO_4 0.33, glucose 10, $CaCl_2$ 1.8, and $CdCl_2$ 0.1, and pH was adjusted to 7.4 with NaOH. The pipettes solution contained (in mM): KCl 150, HEPES 5, EGTA 5, $MgCl_2$ 1, and K_2-ATP 3, and pH was adjusted to 7.3 with KOH. I_{to} was elicited by 500-ms depolarizing steps from −40 mV to +80 mV from a holding potential of −40 mV, with 10-mV increments.

Detection of Calcium Mobilization in Cardiomyocytes in vitro

The calcium mobilizing effect of SiNPs on cardiomyocytes was detected using the Fura-2 fluorescence method. Isolated cardiomyocytes were seeded into 96-well plates at 3.5×10^4 cells/well and cultured for over 24 h. Cells were washed with pre-warmed PBS, and then incubated with Fura-2 AM dissolved in pre-warmed PBS for 37 min at 37°C, followed by three washes with pre-warmed PBS. Cells were exposed to SiNPs (10^{-6} and 2×10^{-4} g/mL) for 60 min, and the cell fluorescence intensities at wavelengths of 340 and 380 nm were detected with a fluorescence microplate reader (BioTek Instruments, USA) after incubation with SiNPs for 5, 15, 30, 45, and 60 min. Cells not exposed to SiNPs served as a negative control. Each experiment was performed in six independent replicates, and three parallel wells were used for each concentration.

Recording of Surface Electrocardiogram

Surface electrocardiograms (ECGs) were recorded to observe the potential arrhythmogenic effects of SiNPs in mice in vivo. Adult male C57BL/6J mice were anesthetized by intraperitoneal injection of 1% phenobarbital sodium (0.005 mL/g bw). The BL-420S physiological data acquisition system (Chendu Taimeng Software Inc, Chengdu, China) was used to record ECGs before exposure to SiNPs (baseline, control), and ECGs were continuously recorded after exposure up to 90 min. Both SiNPs were diluted to desired concentrations with 5% isotonic glucose. SiNP-100 was intravenously (i. v.) injected at doses of 4, 6, 8, and 10 mg/kg and SiNP-20 at 4, 10, 20, and 30 mg/kg. Each mouse received one injection of 100 μL. Arrhythmias were continuously monitored within 90

min after injection. Quantitative analyses of arrhythmias were performed using ANOVA and the chi square test.

Measurement of ROS Generation in vitro

The intracellular ROS assay of cardiomyocytes was performed using a ROS assay kit (Yeasen Biotechnology, Shanghai, China). Cells were loaded with 2,7-dichlorodihydrofluorescein diacetate (DCFH-DA) at 37°C for 20 min, washed with serum-free culture medium for three times, and incubated with SiNP-100 or SiNP-20 at 10^{-8}–10^{-5} g/mL at 37°C for 10 min, followed by at least three washes with fresh culture medium to remove extracellular DCFH-DA. Cells without SiNPs treatment served as a negative control. Cells treated with ROS-up reagent included in the kit served as a positive control. The fluorescence intensity of cells was detected with a fluorescence microplate reader (BioTek Instruments, USA).

Measurement of Lactate Dehydrogenase Leakage in vitro

Lactate dehydrogenase (LDH) leaking from cells was regarded as an indicator of cell membrane injury. The extracellular LDH assay was performed in cultured neonatal ventricular myocytes. Cells were incubated with both SiNPs at 10^{-8}–10^{-5} g/mL for 10 min, washed with PBS, and then the LDH assays were performed using an LDH assay kit (Beyotime Biotechnology, Shanghai, China). Cells without SiNPs treatment served as negative control. Cells treated with LDH release reagent included in the kit served as positive control. Absorbance was detected with an automatic microplate reader (Infinite2000, TECAN, Switzerland) at a wavelength of 490 nm.

ELISA Detection of Myocardial ROS and LDH Levels in Mice in vivo

Adult male C57BL/6J mice were anesthetized by intraperitoneal injection of 1% phenobarbital sodium (0.005 mL/g bw). Both SiNPs were diluted to desired concentrations with 5% isotonic glucose and were i. v. injected. The final serial doses of SiNP-100 were 4, 8, and 10 mg/kg, and those of SiNP-20 were 4, 20, and 30 mg/kg. Each mouse received one injection of 100 μL. Control mice received an injection of 100 μL saline. Five or 60 min after injection, hearts were harvested and myocardial homogenate of each mouse was prepared for ELISA of ROS and LDH. The effects of i. v. SiNPs on myocardial ROS generation and LDH leakage in vivo were measured using the ELISA double antibody sandwich method, and the OD values were read by a microplate reader (BioTek Instruments, USA). Seven mice were tested for each dose of both SiNPs.

Transmission Electron Microscopy

Transmission electron microscopy (TEM) was used to examine the endocytosis and intracellular localization of SiNP-100 and SiNP-20 (both 10^{-6} g/mL) in cultured cardiomyocytes after exposure for 10 min and 1 h, respectively. Cells without SiNP treatment served as control. Cells were then fixed with 2.5% glutaraldehyde in 0.1 M PBS (pH 7.2), washed with PBS, fixed with 1% phosphate-buffered osmium tetroxide, and washed with PBS. Cells were collected and centrifuged at 800 rpm for 5 min. Cell pellets were dehydrated, infiltrated with epoxy resin and acetone, and embedded in epoxy resin. Cells were cut into ultra-thin sections with an ultramicrotome, mounted on copper grids, stained with uranyl acetate and lead citrate, and washed with distilled water. Ultrastructural images of cell sections were taken under a transmission electron microscope (HT7700, HITACHI, Japan).

Statistics

Quantitative data are presented as mean ± standard deviation (SD). Student's *t*-test or ANOVA was used for statistical analysis where appropriate. Numerical data, such as numbers of animals showing arrhythmias, were statistically analyzed using the chi square test. $P < 0.05$ was considered statistically significant.

Results

Characterization of SiNPs

The measured physicochemical characteristics of both SiNPs are summarized in Table 1. SiNP-100 and SiNP-20 exhibited different Z-average sizes and zeta potentials in different media, which may be related to their mild aggregation and medium components sticking to the SiNPs. The polydispersity index (PDI), which indicates the particle size distribution in the medium system, was very low, suggesting a relatively even distribution of the particle size.

SiNP-100 and SiNP-20 Caused Differential Changes in the Transmembrane Potentials of Cardiomyocytes in vitro

Before exposure to SiNPs (baseline), the resting potential (RP) of cardiomyocytes was about −62 mV to −65 mV, and the action potential (AP) exhibited a triangular shape without obvious plateau (Figure 1). Both SiNP-100 and SiNP-20 did not significantly affect the RP, even at the

Table 1 Physicochemical Characterization of SiNPs

Dispersants	Z-Average (nm)/PDI		Zeta Potential (mV)	
	SiNP-100	SiNP-20	SiNP-100	SiNP-20
Ultrapure water	156.1/0.204	31.2/0.508	−37.2	−30.7
Serum-free culture medium	195.3/0.353	66.7/0.633	−12.5	−16.7
Bath solution (AP)	118.3/0.075	160.8/0.532	−18.7	−15.5
Bath solution (I_{K1})	126.7/0.120	88.7/0.570	−18.8	−16.6
Bath solution (I_{Na})	158.9/0.164	40.3/0.361	−11.0	−9.0
Bath solution (I_{to})	117.0/0.271	45.8/0.548	−19.1	−17.2
5% glucose	139.1/0.112	91.1/0.544	−17.1	−18.9

Note: Z-average, mean particle size measured by dynamic laser scattering technology.
Abbreviation: PDI, polydispersity index.

highest tested concentration (10^{-6} g/mL) (Figures 1 and 2). SiNP-100 slightly but significantly increased the APA (Figures 1 and 2A), and significantly prolonged the APD50 and APD90 in a concentration- (10^{-8}–10^{-6} g/mL) and time-dependent manner (Figures 1 and 2A). SiNP-20 at 10^{-8} g/mL did not affect the TMPs (not shown). SiNP-20 at 10^{-7} g/mL did not affect the APA and APD50 (Figures 1 and 2B), but transiently prolonged the APD90 (Figures 1 and 2B), while SiNP-20 at 10^{-6} g/mL significantly decreased the APA and shortened the APD50 and APD90 (Figures 1 and 2B).

SiNPs Had No Effect on the I_{K1} Channel of Cardiomyocytes in vitro

Both SiNP-100 (Figure 3A and C) and SiNP-20 (Figure 3B and D) at the highest tested concentration (10^{-6} g/mL) did not significantly affect the I_{K1} currents and current densities, and did not affect the activation kinetics of I_{K1} channels of cardiomyocytes (Figure 3E and F).

SiNP-100 and SiNP-20 Exerted Diverse Effects on the Voltage-Gated Na^+ Channel of Cardiomyocytes in vitro

The about results showed that SiNPs differentially affected the AP depolarization of cardiomyocytes as indicated by the APA, and the I_{Na} channel is known responsible for the depolarization. We therefore tested the effects of SiNPs on the I_{Na} channel of cardiomyocytes. Results showed that within 30 min after exposure, SiNP-100 at 10^{-6} g/mL significantly increased the I_{Na} currents (Figure 4A) and current densities as indicated by the I–V curves (Figure 4C), while SiNP-20 at 10^{-6} g/mL decreased the I_{Na} currents (Figure 4B) and current densities (Figure 4D) compared to baseline. Both SiNPs shifted the activation curves of I_{Na} channels in a leftward direction compared with control (Figure 4E and F), suggesting that SiNPs accelerate the activation of I_{Na} channels, or in other words, I_{Na} channels are activated at more negative membrane potentials after exposure to SiNPs. Both SiNPs accelerated the inactivation of I_{Na} channels in ventricular myocytes, but for SiNP-100 this effect did not reach statistical significance (Figure 5). These differential effects of SiNP-100 and SiNP-20 on I_{Na} channels were consistent with their respective effects on the depolarization of AP.

SiNP-100 and SiNP-20 Had Contrary Effects on the I_{to} Channel of Cardiomyocytes in vitro

SiNP-100 at 10^{-6} g/mL decreased the I_{to} currents and current densities of cardiomyocytes (Figure 6A and C), while SiNP-20 at 10^{-6} g/mL increased the I_{to} currents and current densities (Figure 6B and D). Both SiNP-100 and SiNP-20 did not significantly affect the activation kinetics of I_{to} channels (Figure 6E and F). The contrary effects of SiNP-100 and SiNP-20 on I_{to} channels could partially explain their diverse effects on the APD.

SiNPs Induced Calcium Mobilization in Cardiomyocytes in vitro

Compared with control cells, cardiomyocytes exposed to SiNP-100 and SiNP-20 at 10^{-6} g/mL showed significant elevations in the Fura-2 fluorescence 340/380 ratio within 60 min after exposure (Figure 7), and there was no significant difference in the 340/380 ratios between SiNP-100-treated and SiNP-20-treated cells. SiNP-100 and SiNP-20 at a higher concentration (2×10^{-4} g/mL) induced larger 340/380 ratio than at 10^{-6} g/mL (Figure 7). These results suggest that both SiNP-100 and SiNP-20 induced calcium mobilization in cardiomyocytes to a similar extent.

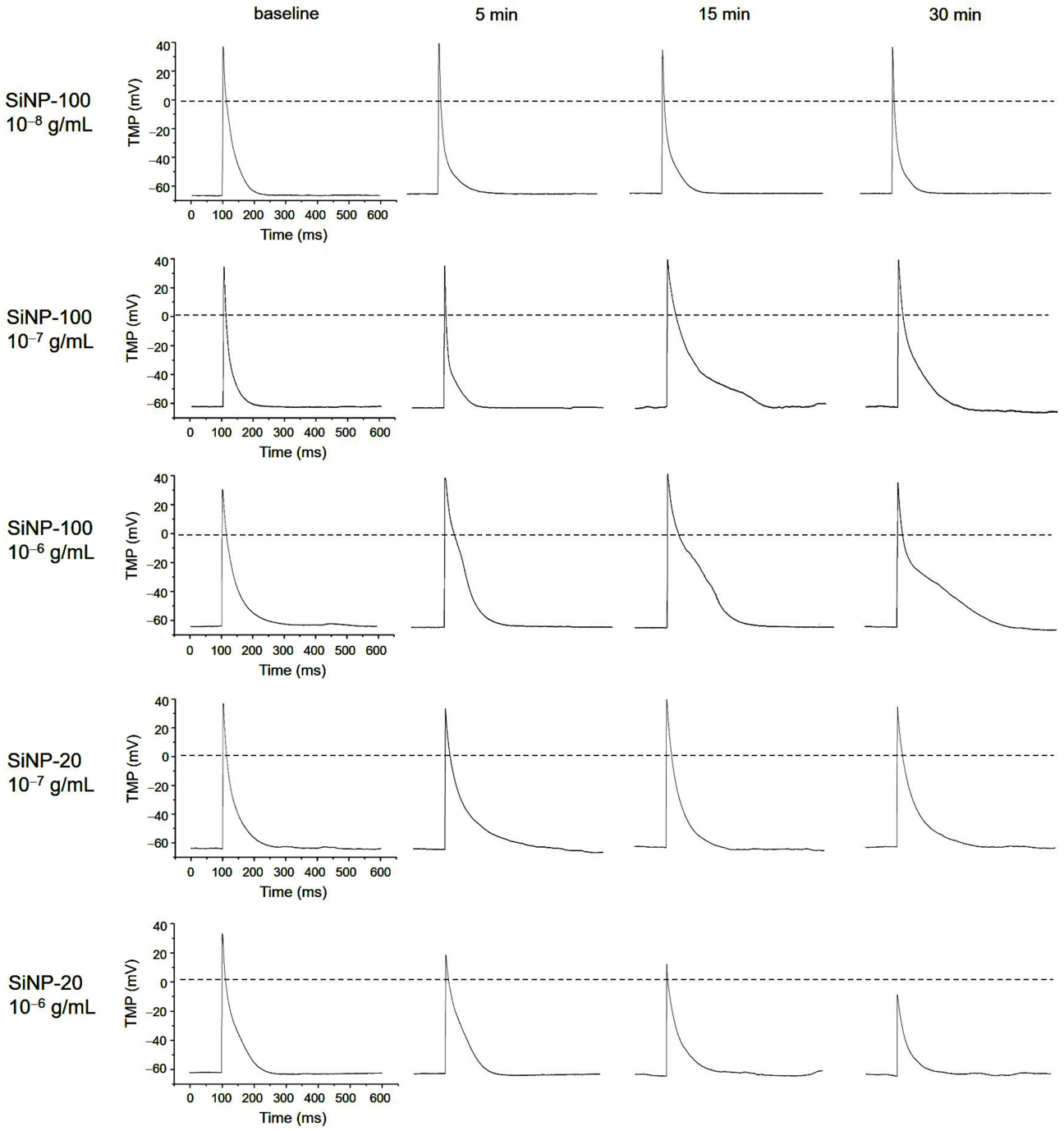

Figure 1 Representative recordings showing the effects of SiNP-100 and SiNP-20 on the transmembrane potential (TMP) of cultured neonatal mice ventricular myocytes. Note that both SiNPs did not affect the resting potential (RP), but substantially affected the action potential (AP) in a concentration- and time-dependent manner. SiNP-20 at 10^{-8} g/mL had no effect on the TMP (not shown).

SiNPs Induced Non-Lethal Tachyarrhythmias and Lethal Bradyarrhythmias in Mice in vivo

The above results showed the differential effects of SiNPs on the depolarization and repolarization of APs of cardiomyocytes and the underlying ion channel mechanisms. Based on these results and the known mechanisms of arrhythmias, we hypothesized that SiNPs might induce both tachyarrhythmias and bradyarrhythmias, depending on particle size, exposure dose, and exposure time. The representative ECGs before and after exposure to SiNPs are shown in Figure 8, and the statistical summary of arrhythmias is shown in Table 2. SiNP-100 (i. v.) at 4–6 mg/kg accelerated the sinus heart rate (HR), and one

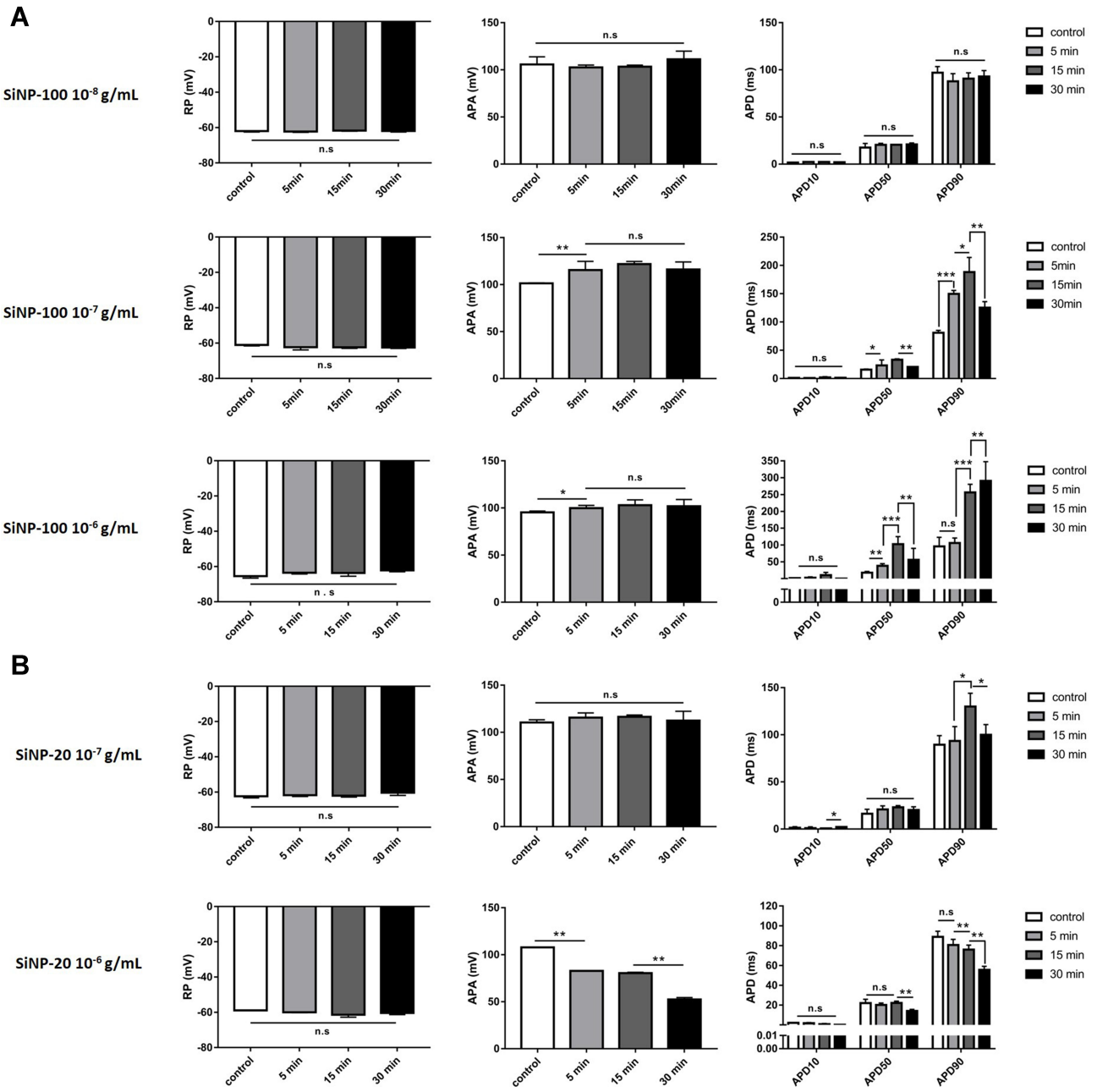

Figure 2 Statistical results showing the acute effects of SiNPs on the TMP parameters of mouse cardiomyocytes in vitro. (**A**) SiNP-100 at 10^{-8}–10^{-6} g/mL and exposure for 5–30 min. (**B**) SiNP-20 at 10^{-7} and 10^{-6} g/mL and exposure for 5–30 min. *P<0.05, **P<0.01, ***P<0.001, n=5 cells for each SiNP concentration.

of the four tested mice developed bradyarrhythmia and cardiac asystole within the observed 90 min (Figure 8 (left) and Table 2). SiNP-100 at 8 mg/kg gradually decreased the sinus HR, prolonged the P-R intervals, and induced complete atrio-ventricular conduction block (AVB) at about 80–90 min after exposure (Figure 8 (left)), and two of six mice died of cardiac asystole within 90 min (Table 2). SiNP-100 at 10 mg/kg sequentially induced sinus tachycardia, premature ventricular contraction (PVC), and complete AVB, and two of six mice died of cardiac asystole within 65 min after exposure (Figure 8 (left) and Table 2).

SiNP-20 (i. v.) at 4 and 10 mg/kg did not affect the ECG (Figure 8 (right)); at 20 mg/kg, it only induced sinus tachycardia within 90 min after exposure (Figure 8 (right)); but at 30 mg/kg sequentially induced sinus tachycardia, ventricular tachycardia (VT), complete AVB, and two of four animals died of cardiac asystole within 60 min after exposure (Figure 8 (right) and Table 2).

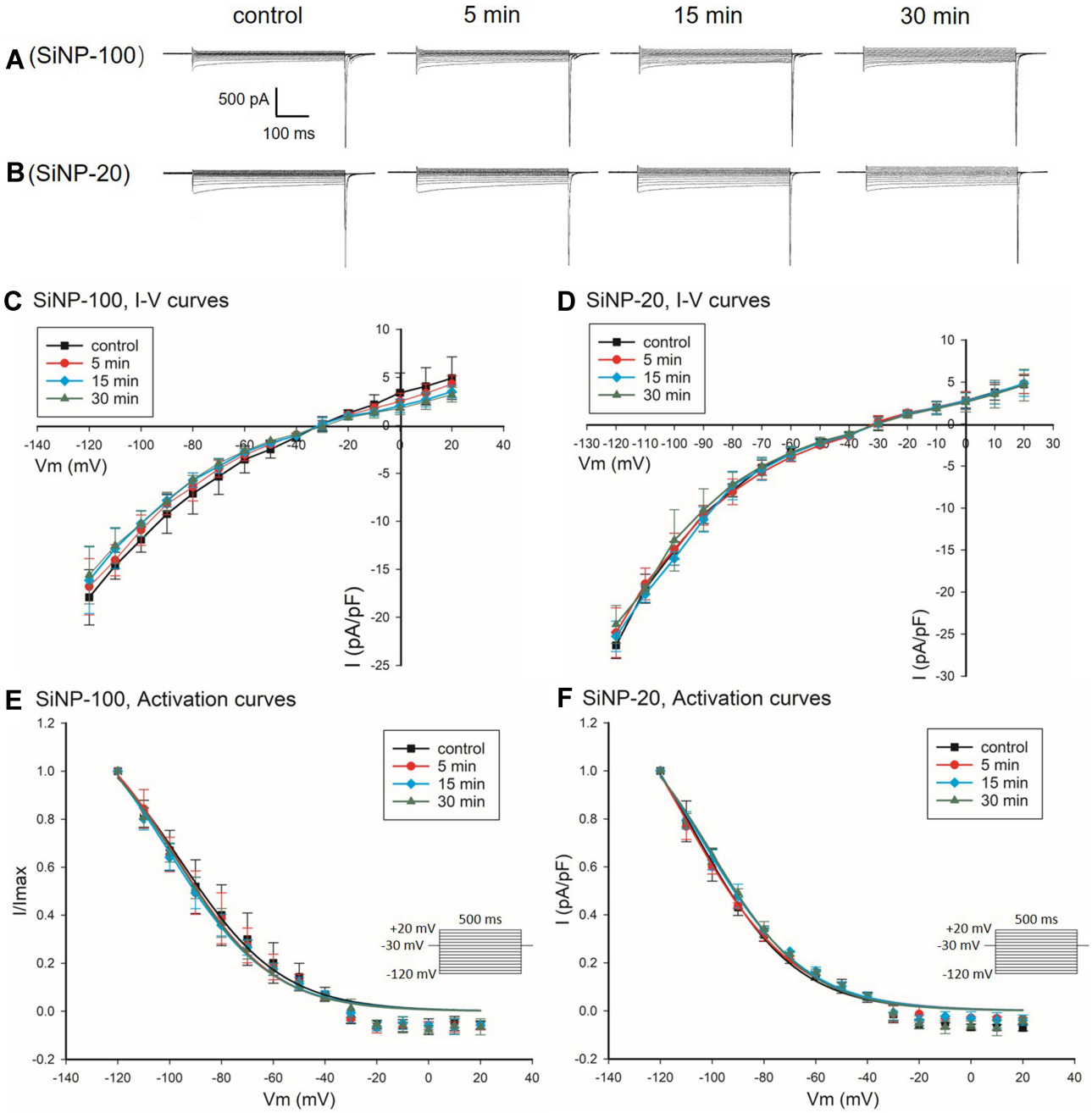

Figure 3 Effects of SiNP-100 and SiNP-20 (both 10^{-6} g/mL) on the I_{K1} channels of cultured neonatal mice ventricular myocytes. (**A** and **B**) typical I_{K1} current tracings at baseline and after exposure to SiNP-100 and SiNP-20 for 5–30 min. (**C** and **D**) corresponding I–V curves of I_{K1} channels at baseline (control) and after exposure to SiNP-100 and SiNP-20, respectively. (**E** and **F**) activation curves of I_{K1} channels at baseline and after exposure to SiNP-100 and SiNP-20, respectively. N=5 cells for each SiNP concentration.

From the above ECG results, it is obvious that both SiNPs were arrhythmogenic and could cause sudden cardiac death at higher doses due to serious bradyarrhythmias which finally developed to cardiac asystole within the observed 90 min. The cardiac electrophysiological toxicity of SiNP-100 was higher than that of SiNP-20. The lowest toxic doses for SiNP-100 and SiNP-200 were 4 mg/kg and 20 mg/kg, respectively, and the lethal doses were approximately 6–8 mg/kg and 30 mg/kg (i. v.) for SiNP-100 and SiNP-200, respectively, in adult mice in vivo.

Acute Exposure to SiNPs Did Not Elevate ROS Generation and LDH Leakage in Cardiomyocytes in vitro

Both SiNPs at 10^{-8}–10^{-5} g/mL for 10 min did not increase the intracellular ROS levels (Figure S1) or the

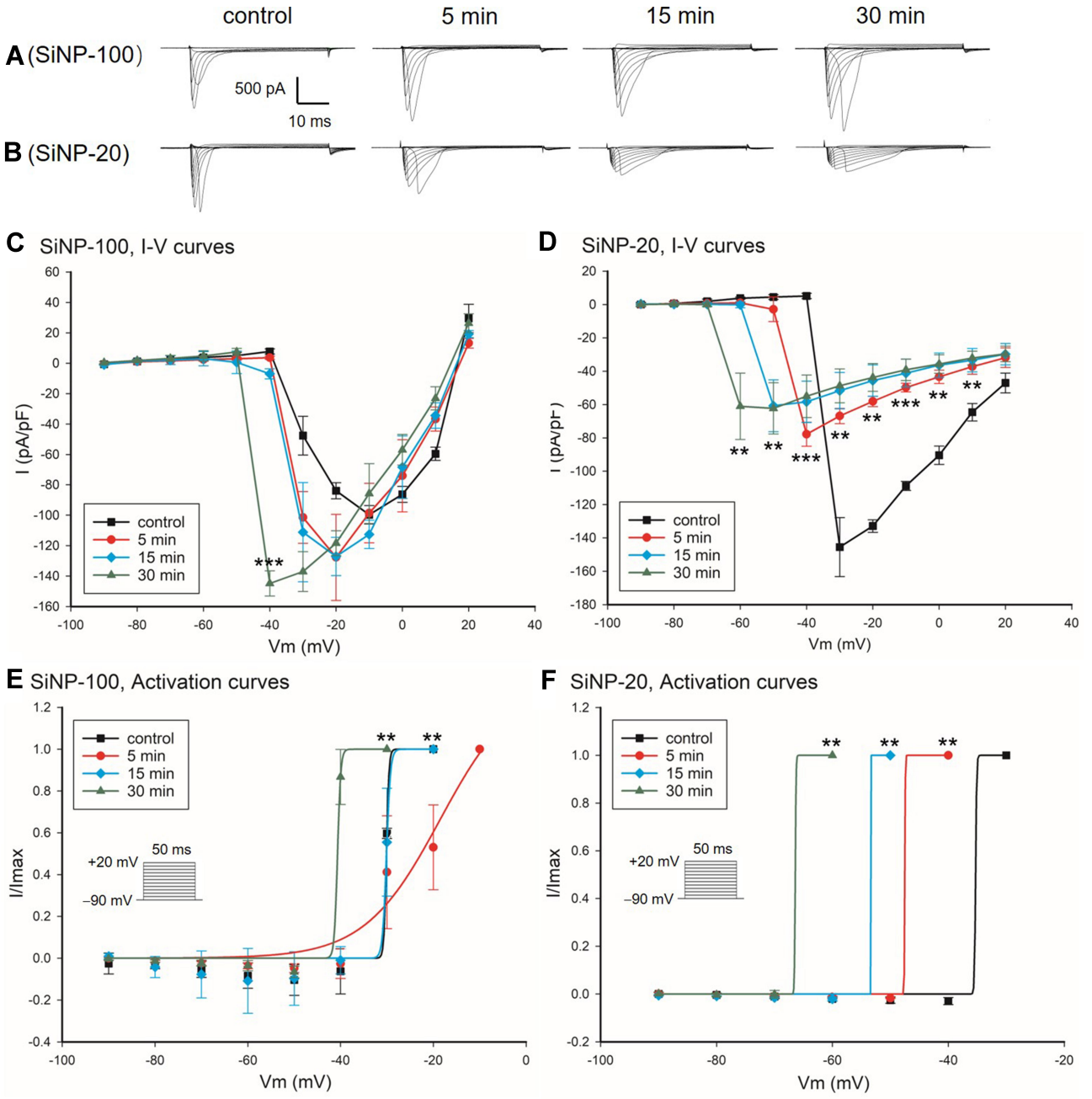

Figure 4 Effects of SiNP-100 and SiNP-20 (both 10^{-6} g/mL) on the I_{Na} channels of cultured neonatal mice ventricular myocytes. (**A** and **B**) typical I_{Na} currents recorded at baseline and after exposure to SiNP-100 or SiNP-20 for 5–30 min. (**C** and **D**) corresponding I–V curves of I_{Na} channels at baseline and after exposure to SiNP-100 and SiNP-20, respectively. **P<0.01, ***P<0.001 vs baseline (control). (**E** and **F**) activation curves of I_{Na} channels at baseline and after exposure to SiNP-100 and SiNP-20, respectively. N = 6 cells for each SiNP concentration.

extracellular LDH levels (Figure S1) compared to control cardiomyocytes. The ROS-up reagent and LDH-releasing reagent (positive controls) significantly increased the intracellular ROS level and the extracellular LDH level, respectively (Figure S1). These results suggest that the acute toxic effects of SiNPs on cardiac electrophysiology are not associated with oxidative stress and membrane damage in cardiomyocytes in vitro.

Acute Exposure to SiNPs Did Not Increase Myocardial ROS Levels, but Increased LDH Levels in a Dose- and Exposure Time-Dependent Manner in Mice in vivo

SiNP-100 at 4, 8, and 10 mg/kg and SiNP-20 at 4, 20, and 30 mg/kg did not significantly increase the myocardial ROS levels after i. v. exposure for 5 min and 60 min

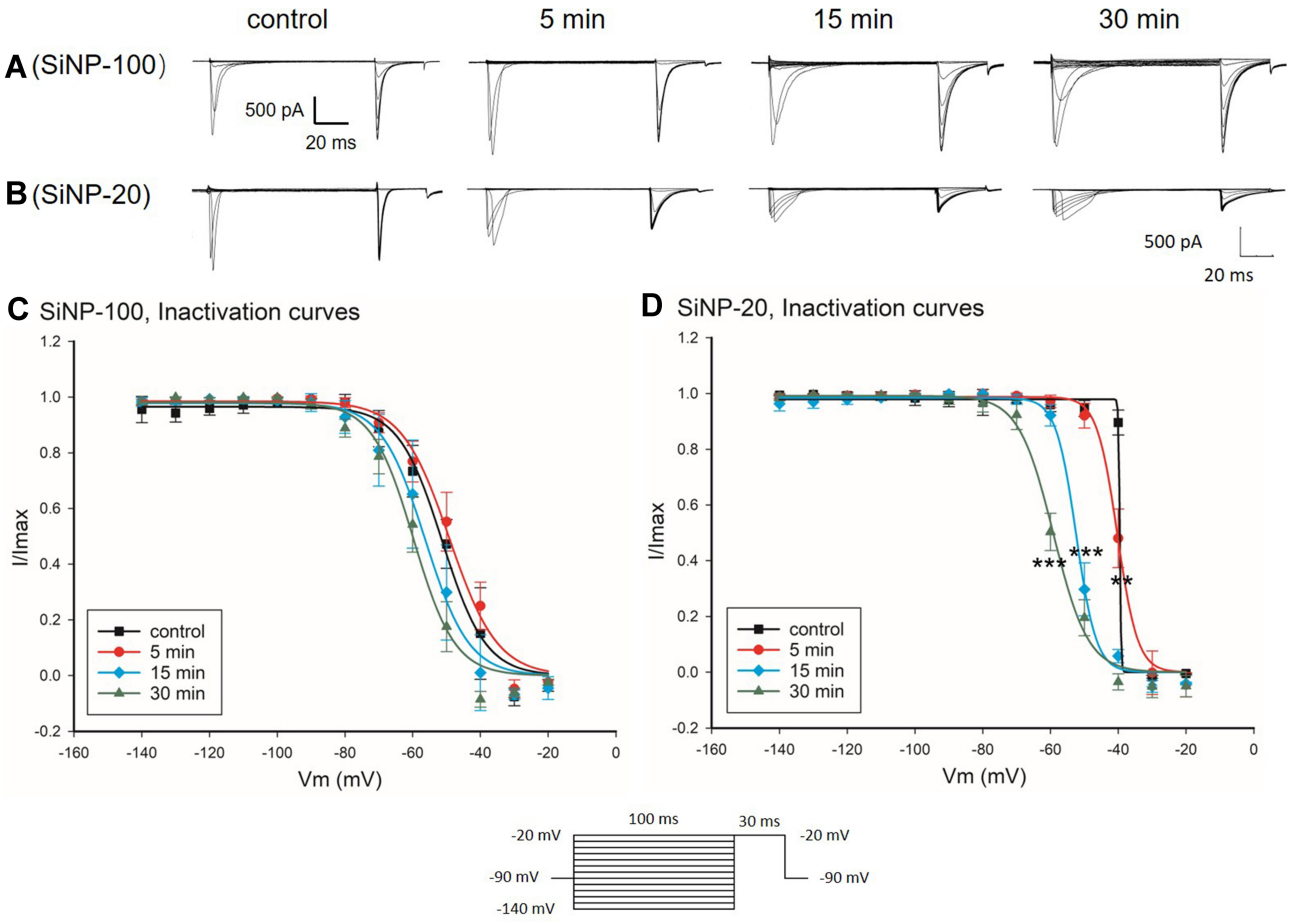

Figure 5 Effects of SiNP-100 and SiNP-20 (both 10^{-6} g/mL) on the inactivation kinetics of I_{Na} channels in cultured neonatal mice ventricular myocytes. (**A** and **B**) typical I_{Na} induced by the stimulating protocol for checking inactivation at baseline and after exposure to SiNP-100 and SiNP-20 for 5–30 min. (**C** and **D**) inactivation curves of I_{Na} channels at baseline (control) and after exposure to SiNP-100 and SiNP-20, respectively. **P<0.01, ***P<0.001 vs control, n=6 cells for each SiNP concentration.

(Figure S2). SiNP-20 at 4 mg/kg even significantly decreased the myocardial ROS levels after exposure for 5 min and 60 min (Figure S2). Both SiNP-100 and SiNP-20 did not significantly increase myocardial LDH levels at lower doses and/or shorter exposure times (Figure S2), but significantly increased myocardial LDH levels at the higher doses and/or longer exposure times (Figure S2).

The Rapid Toxic Effects of SiNPs on Cardiomyocyte Electrophysiology Were Endocytosis-Independent in vitro

TEM results showed that both SiNPs (10^{-6} g/mL) were not endocytosed within 10 min after exposure, but were endocytosed 1 h after exposure by cardiomyocytes (Figure 9), suggesting that the acute toxicities of SiNPs on the electrophysiology of cardiomyocytes are endocytosis-independent, because SiNPs began to affect the TMPs and ion channels usually within 5 min after exposure in vitro.

Discussion

SiNPs have emerged as a promising therapy vector for heart diseases. However, their potential cardiac toxicity and functional mechanisms remain poorly understood, especially the toxicity on cardiac electrophysiology and heart rhythm. The present study focused on this issue both in vitro and in vivo and demonstrated that SiNPs have significant acute toxic effects on the TMPs and ion channels of cardiomyocytes and, importantly, could induce lethal bradyarrhythmias depending on particle size and dose and exposure time.

We first demonstrated that both SiNPs had no effect on the RP of cardiomyocytes in vitro. This character of SiNPs is different from some other types of nanoparticles such as silver nanoparticles[22] and platinum nanoparticles[23] which can depolarize the RP of cardiomyocytes. As the I_{K1} channel is the dominant ion channel in the maintenance of the RP,[24] we therefore hypothesized and verified that SiNPs had no effect on the I_{K1} channel of cardiomyocytes.

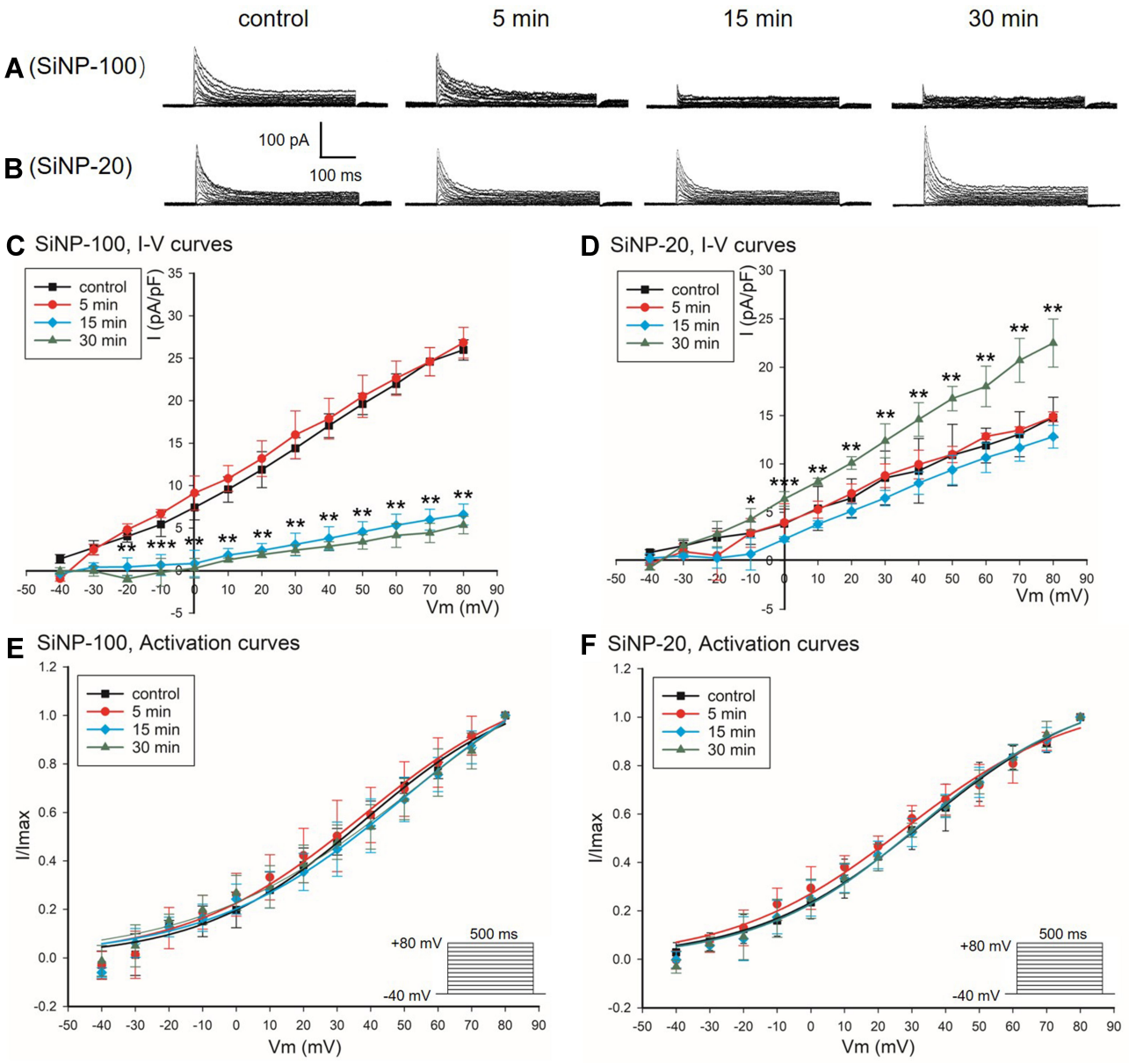

Figure 6 Effects of SiNP-100 and SiNP-20 (both 10^{-6} g/mL) on the I_{to} channels in cultured neonatal mice ventricular myocytes. (**A** and **B**) typical I_{to} currents at baseline (control) and after exposure to SiNP-100 and SiNP-20, respectively, for 5–30 min. (**C** and **D**) corresponding I–V curves of I_{to} channels at baseline and after exposure to SiNP-100 and SiNP-20, respectively. (**E** and **F**) activation curves of I_{to} channels at baseline and after exposure to SiNP-100 and SiNP-20, respectively. *P<0.05, **P<0.01, ***P<0.001 vs control. N = 7 cells for each SiNP concentration.

This finding also suggests that the arrhythmogenic effects of SiNPs are not associated with the RP and I_{K1} channel.

We then examined the effects of SiNPs on the depolarization of AP and the responsible I_{Na} channels in cardiomyocytes in vitro. SiNP-100 slightly increased the APA but SiNP-20 decreased it. Consistent with this finding, SiNP-100 increased but SiNP-20 decreased the I_{Na} current density. These results verified the effects and mechanism of SiNPs on AP depolarization. In addition, both SiNPs accelerated the activation and inactivation of I_{Na} channels with minor difference. The different effects of SiNP-100 and SiNP-20 on depolarization, I_{Na} current density, and I_{Na} channel kinetics may be associated with their differential arrhythmogenic effects in vivo.

The effects of SiNPs on AP repolarization were a bit complicated and depended on particle size, concentration, and exposure time (shown in Figures 1 and 2). SiNP-100 prolonged the APD50 and APD90 at higher concentrations and longer exposure times, while SiNP-20 either prolonged the APD50 and APD90 or shortened them, depending on the concentration and exposure time. It is known that APD decides the effective refractory period (ERP) at

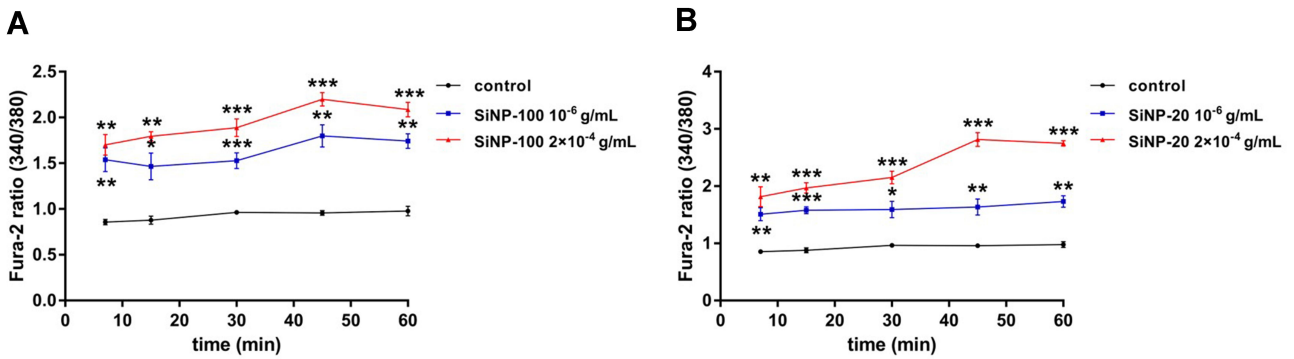

Figure 7 The calcium mobilizing effects of SiNPs on cultured neonatal mice cardiomyocytes in vitro. Cardiomyocytes were loaded with Fura-2AM and then exposed to SiNPs at serial concentrations and different exposure times. The fluorescence intensities at 340/380 nm were detected with a fluorescence microplate reader. (**A**) SiPN-100. (**B**) SiNP-20. *P<0.05, **P<0.01, ***P<0.001 vs control. Each experiment was performed in six independent replicates, and three parallel wells were used for each concentration.

physiological conditions, and altered ERP affects the excitation conduction route and favors the occurrence of reentry and conduction block; therefore, the effects of SiNPs on AP repolarization, together with their effects on AP depolarization, may explain why SiNPs induced both tachyarrhythmias or bradyarrhythmias. However, the effects of SiNP-100 and SiNP-20 on the APD did not perfectly match their effects on the repolarizing K^+ currents, perhaps due to different experimental conditions in which the particle Z-sizes were different in vitro. Notably, we observed that the SiNP-induced tachyarrhythmias were non-lethal because SiNPs could not induce ventricular fibrillation (VF), while the induced bradyarrhythmias were lethal due to cardiac systole in mice.

We further investigated the ion channel-related mechanisms underlying the effects of SiNPs on AP repolarization. A variety of ion channels are involved in the AP repolarization of neonatal ventricular myocytes.[25] AP repolarization depends on the activity balance of the outward K^+ channel currents which accelerate repolarization and the inward $I_{Ca\text{-}L}$ channel currents which decelerate repolarization and create a plateau in the repolarizing phase of cardiomyocytes. The K^+ channels responsible for repolarization mainly include I_{K1}, I_{to}, and I_K (including I_{Kr} and I_{Ks} components) channels. I_K channels have been found to be rapidly downregulated after birth and are not expressed in adult mouse ventricular myocytes.[26] Because SiNPs did not affect the I_{K1} channel of mice cardiomyocytes in the present study and due to the low or absent expression of I_K channel in mice after birth,[26] the I_{to} channel may be the major ion channel to accelerate repolarization in mouse cardiomyocytes. We found that SiNP-100 decreased but SiNP-20 increased the I_{to} current densities; these diverse effects of SiNP-100 and SiNP-20 on I_{to} channels may at least partially explain their different effects on the APD.

The $I_{Ca\text{-}L}$ channel plays important roles in AP repolarization and AP shaping of cardiomyocytes and in triggering calcium mobilization and arrhythmias. It has been reported that $I_{Ca\text{-}L}$ channels are expressed in mice hearts and the expression is elevated after birth under the stimulation of the sympathetic nerve derived neuropeptide Y.[27] However, mouse cardiomyocytes show a triangular AP shape and a very short APD, which suggests low expression levels of the $I_{Ca\text{-}L}$ channel compared with larger animals and humans. We observed that both SiNPs could induce calcium mobilization to a similar extent (shown in Figure 7), suggesting that $I_{Ca\text{-}L}$ channel is expressed in neonatal cardiomyocytes, and both SiNPs activate the $I_{Ca\text{-}L}$ channel and induce calcium mobilization via the Ca^{2+}-induced Ca^{2+} release mechanism. It is rational to speculate that activation of $I_{Ca\text{-}L}$ channels by SiNPs may contribute to SiNP-induced arrhythmias. Alternative studies have indicated that SiNPs (i) induce cardiac dysfunction and bradycardia via the neutrophil-mediated cardiac inflammation in zebrafish embryos,[16] (ii) exert toxic effect on isolated adult cardiomyocytes via impairment of mitochondrial function and Ca^{2+} homeostasis,[19] and (iii) induce cardiac dysfunction via the opening of the mitochondrial permeability transition pore in rat heart and human cardiomyocytes.[28] These findings suggest that dysfunction of mitochondria and Ca^{2+} homeostasis in cardiomyocytes and myocardial inflammation plays important role in the cardiac toxicity of SiNPs. The present study further demonstrated that the hazardous effects of

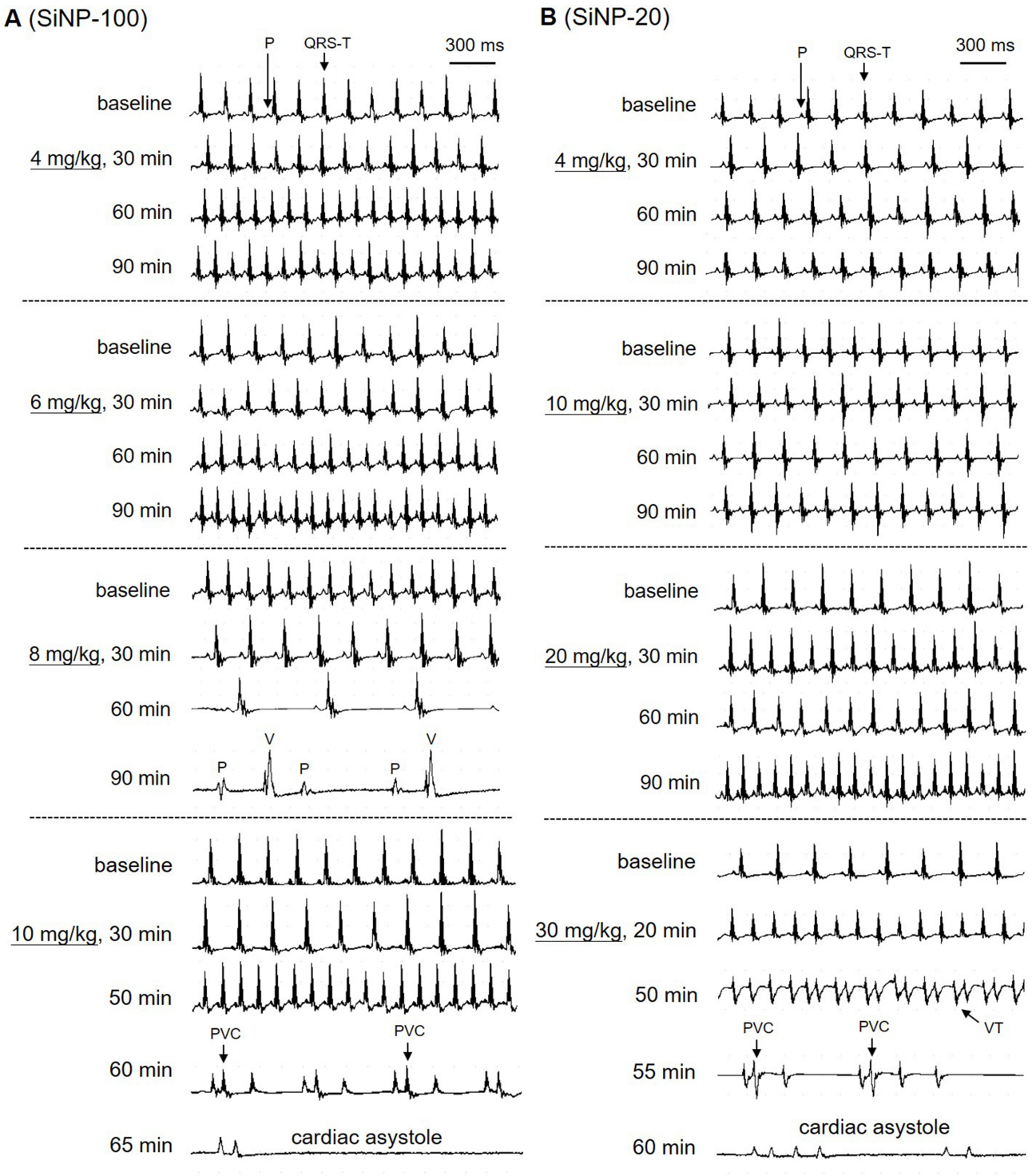

Figure 8 Typical ECGs showing the arrhythmogenic effects of SiNP-100 (**A**) and SiNP-20 (**B**) in adult mice in vivo. Both SiNP-100 and SiNP-20 induced sinus tachycardia, ventricular tachyarrhythmias (PVC or VT), complete atrio-ventricular conduction block (AVB), cardiac asystole and sudden cardiac death in a dose- and time-dependent manner. Note that the dose of SiNP-100 (6 mg/kg) was much lower than the dose of SiNP-20 (30 mg/kg) beginning to induce cardiac asystole, suggesting that SiNP-100 was more toxic than SiNP-20.

Abbreviations: P, P wave; R, R wave; QRS-T, QRS complex and T wave; V, ventricular escape rhythm; PVC, premature ventricular contractions; VT, ventricular tachycardia.

SiNPs on several ion channels and AP are also important mechanisms underlying the arrhythmogenic effects of SiNPs.

In addition, we investigated whether the effects of SiNPs on cardiac electrophysiology and arrhythmogenesis are associated with ROS generation and membrane

Table 2 Statistical Summary of Cardiac Arrhythmias within 90 min After Intravenous Exposure to SiNPs in Mice in vivo

	N	Incidence of Arrhythmias	Episodes of PVC	Incidence of VT	Incidence of AVB	Incidence of Cardiac Asystole
Control	5	0/5	0±0	0/5	0/5	0/5
SiNP-100, 4 mg/kg	4	1/4	13±2**	0/4	0/4	0/4
SiNP-100, 6 mg/kg	4	2/4	15±5**	0/4	1/4	1/4
SiNP-100, 8 mg/kg	6	4/6*	0±0	0/6	3/6	2/6
SiNP-100, 10 mg/kg	6	5/6*	6±3	2/6	2/6	2/6
SiNP-20, 4 mg/kg	4	0/4	0±0	0/4	0/4	0/4
SiNP-20, 20 mg/kg	4	1/4	0±0	0/4	0/4	0/4
SiNP-20, 30 mg/kg	4	3/4*	47±10**	3/4*	1/4	2/4

Notes: *P < 0.05, **P < 0.01 vs respective controls.
Abbreviations: PVC, premature ventricular contraction; VT, ventricular tachycardia; AVB, complete atrio-ventricular conduction block.

damage, as indicated by LDH leaking. Previous studies revealed that oxidative stress and membrane injury are important mechanisms of SiNP cytotoxicity.[29,30] The present study showed that SiNPs could rapidly affect the AP and ion channels of cardiomyocytes (within 5 min), while SiNPs could not elevate cell ROS generation and LDH leaking within 10 min, suggesting that the acute toxic effects of SiNPs are oxidative stress- and membrane injury-independent in vitro. In vivo, SiNPs also did not increase myocardial ROS level within 60 min, but increased LDH leakage at higher doses and/or longer exposure times. These results suggest that SiNPs can directly interfere with the activities of ion channels at the extracellular side, but in vivo, more factors may be involved in the effects of SiNPs on cardiac toxicity, especially after longer exposure times. Furthermore, TEM results showed that SiNPs were not endocytosed by cardiomyocytes within 10 min after exposure which suggests that the acute effects of SiNPs on cardiomyocyte electrophysiology are endocytosis-independent, at least in vitro. In vivo, the endocytosis of SiNPs by cardiomyocytes may partially contribute to the cardiac toxicity, including arrhythmogenesis, especially at higher doses and longer exposure times.

It is considered that the toxicity of SiNPs is size-dependent; smaller particles are usually more toxic than bigger ones in some cells. For example, the DNA damaging effects of SiNPs in human umbilical vein endothelial cells (HUVECs) showed a negative size-dependent relationship,[31] and the thrombocytopenia, liver damage, and lethal toxicity of i. v. administrated SiNPs in mice also showed negative correlations with particle sizes.[32] However, we identified that SiNPs with a larger size (SiNP-100) exerted higher toxicity than the smaller ones (SiNP-20) on cardiac electrophysiology; the lowest doses of SiNP-100 and SiNP-20 beginning to affect heart rate or rhythm were 4 mg/kg and 20 mg/kg, respectively, in mice in vivo. We reported recently that the toxicity of SiNP-100 on HUVECs is higher than that of SiNP-20.[33] This may be associated with the faster sedimentation of SiNP-100 onto the cell surface than that of SiNP-20, as identified using the in vitro Sedimentation, Diffusion and Dosimetry (ISDD) model.[33,34]

In addition, other physical characteristics of nanoparticles, such as the zeta potential, may also contribute to the biotoxicity of nanoparticles. The zeta potential predicts the physical stability of the nanosuspension, the higher the absolute value of zeta potential, the higher the dispersion of nanoparticles in a solution. We showed that the zeta potentials of SiNPs were all negative and were different in different media, with the highest in ultrapure water (Table 1). The smaller zeta potentials in experimental solutions and perhaps also in the body fluid (not determined) suggest that SiNPs may aggregate to some extent, and the aggregated form might also contribute to the cardiac toxicity.

Limitations and Future Perspectives

The first limitation of the study is that we did not examine the effects of SiNPs on the $I_{Ca\text{-}L}$ channel, which is known to participate in the AP repolarization of cardiomyocytes. Instead, we observed the calcium mobilizing effects of both SiNPs, which suggest that Ca^{2+} homeostasis is involved in SiNP-induced arrhythmias. A second limitation is that we did not check the effects of SiNPs on the ion channels of the sinus node, the atrio-ventricular node, and Purkinje fibers of the heart; these effects may also contribute to the arrhythmogenic effects of SiNPs in vivo. A third limitation is that we could not extrapolate the

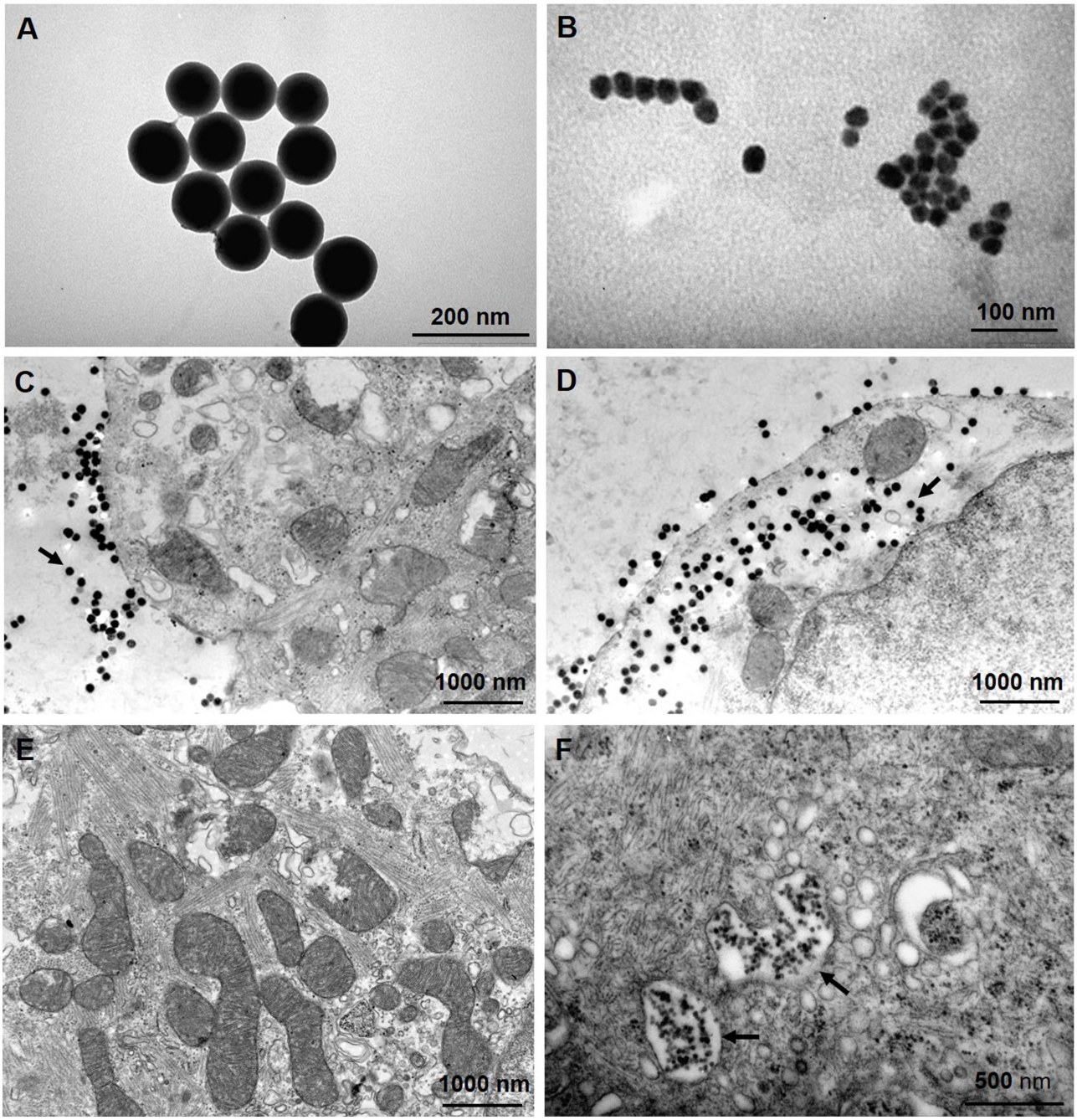

Figure 9 TEM images showing the morphology of SiNPs and their endocytosis by cultured neonatal mice ventricular myocytes. (**A** and **B**) TEM images of SiNP-100 and SiNP-20 in culture medium. (**C**) cells exposing to SiNP-100 for 10 min, SiNP-100 located at the extracellular space (arrow), and no endocytosis was observed. (**D**) cells exposing to SiNP-100 for 1 h, substantial amounts of SiNP-100 were observed inside the cell (arrow). (**E**) cell exposing to SiNP-20 for 10 min, no SiNP-20 endocytosis was observed. (**F**) cell exposing to SiNP-20 for 1 h, SiNP-20 was endocytosed and located mainly inside vesicles (arrows).

accurate toxic dose range of SiNPs in humans based on cell and animal studies. However, although we did not measure the actual blood levels of SiNPs after i. v. injection in mice, we calculated that the blood levels of SiNPs needed to induce arrhythmias in mice in vivo are much higher (at least three orders of magnitude) than the levels needed to affect AP and ion channels of cardiomyocytes in vitro. The reasons for this difference might be that the i. v. infused SiNPs could quickly diffuse out of capillaries, sediment on the cell surface, and be engulfed by cells at in vivo conditions; these processes would quickly reduce the blood SiNP levels, and thus higher initial SiNP doses are needed to maintain toxic blood levels for inducing arrhythmias. Of course, actual measurements of the

blood SiNP levels would be more accurate than estimations.

In certain circumstances of human exposure to SiNPs, we should pay close attention to the arrhythmogenic effects of SiNPs besides other hazardous effects of SiNPs. Thus, the severity and toxicity of SiNPs for humans need to be determined in the future. A better control of human exposure may benefit the appropriate utilization of SiNPs in many fields. In addition, we need to acquire more knowledge about the damages of SiNPs to animal health and ecology in order to keep a good balance between benefits and harms of this nanomaterial.

Conclusion

SiNPs exert profound acute toxic effects on cardiac electrophysiology at the molecular, cellular, and integrative levels. Both SiNPs do not affect the RP of cardiomyocytes in vitro, as they do not affect the I_{K1} channel. SiNP-100 and SiNP-20 exert diverse effects on AP depolarization and repolarization: SiNP-100 enhances depolarization by enhancing I_{Na} currents and delays repolarization by repressing the I_{to} channel, while SiNP-20 suppresses depolarization by decreasing I_{Na} currents and concentration-dependently delays or accelerates repolarization by affecting the I_{to} channel and certain unknown factor-(s). In vivo, both SiNPs induce non-lethal tachyarrhythmias and lethal bradyarrhythmias in mice in a dose- and time-dependent manner. SiNP-100 is more toxic than SiNP-20 both in vitro and in vivo. The lowest toxic doses in vivo are about 4 mg/kg and 20 mg/kg for SiNP-100 and SiNP-20, respectively. These acute toxic effects of SiNPs on cardiac electrophysiology are not associated with cardiomyocyte ROS generation both in vitro and in vivo, but more factors may be involved in vivo. The study provides new information and warnings with respect to the utilization of SiNPs in the fields of nanobiology and nanomedicine.

Statement of Ethics Approving Committee and the Approval Number

The animal use protocol was approved by the Ethics Committee of Southwest Medical University for animal experiments (approval No. 201705-093). The used cardiomyocytes were isolated from the experimental animals.

Acknowledgments

This work was supported by grants from the National Natural Science Foundation of China (NSFC) (81670313 to JC, 81870261 to GL), the Sichuan Science and Technology Program (2019YJ0472 to PZ), the Luzhou Science and Technology Program (2018LZXNYD-ZK44 to PZ), Collaborative Innovation Center for Prevention and Treatment of Cardiovascular Disease of Sichuan Province, Southwest Medical University (xtcx-2016-11 to PZ), and Shanxi "1331 Project" Key Subjects Construction (1331KSC to JC). We thank LetPub (www.letpub.com) for its linguistic assistance during the preparation of this manuscript.

Author Contributions

All authors made a significant contribution to the work reported, whether that is in the conception, study design, execution, acquisition of data, analysis and interpretation, or in all these areas; took part in drafting, revising or critically reviewing the article; gave final approval of the version to be published; have agreed on the journal to which the article has been submitted; and agree to be accountable for all aspects of the work.

Disclosure

The authors report no conflicts of interest in this work.

References

1. Fukata N, Subramani T, Jevasuwan W, Dutta M, Bando Y. Functionalization of silicon nanostructures for energy-related applications. *Small*. 2017;13(45):1701713. doi:10.1002/smll.201701713
2. Li J, Qiu C, Fan H, Bai Y, Jin Z, Wang J. A novel cyclodextrin-functionalized hybrid silicon wastewater nano-adsorbent material and its adsorption properties. *Molecules*. 2018;23(6):1485. doi:10.3390/molecules23061485
3. Soengas R, Navarro Y, Iglesias MJ, Ortiz L. Immobilized gold nanoparticles prepared from gold (III)-containing ionic liquids on silica: application to the sustainable synthesis of propargylamines. *Molecules*. 2018;23(11):2975. doi:10.3390/molecules23112975
4. Paramsothy M. Alleviating climate change and pollution with nanomaterials. *Nanomaterials (Basel)*. 2020;10(2):358. doi:10.3390/nano10020358
5. Aly I, Taher EE, El Nain G, et al. Advantages of bioconjugated silica-coated nanoparticles as an innovative diagnosis for human toxoplasmosis. *Acta Trop*. 2018;177:19–24. doi:10.1016/j.actatropica.2017.09.024
6. Park SM, Aalipour A, Vermesh O, Yu JH, Gambhir SS. Towards clinically translatable in vivo nanodiagnostics. *Nat Rev Mater*. 2017;2:17014. doi:10.1038/natrevmats.2017.14
7. Chen F, Zhang X, Ma K, et al. Melanocortin-1 receptor-targeting ultrasmall silica nanoparticles for dual-modality human melanoma imaging. *ACS Appl Mater Interfaces*. 2018;10(5):4379–4393. doi:10.1021/acsami.7b14362
8. Shi M, Xia L, Chen Z, et al. Europium-doped mesoporous silica nanosphere as an immune-modulating osteogenesis/angiogenesis agent. *Biomaterials*. 2017;144:176–187. doi:10.1016/j.biomaterials.2017.08.027
9. Watermann A, Brieger J. Mesoporous silica nanoparticles as drug delivery vehicles in cancer. *Nanomaterials (Basel)*. 2017;7:185. doi:10.3390/nano7070189

10. Shirshahi V, Soltani M. Solid silica nanoparticles: applications in molecular imaging. *Contrast Media Mol Imaging*. 2014;10:1–17. doi:10.1002/cmmi.1611
11. Wang Y, Zhao Q, Han N, et al. Mesoporous silica nanoparticles in drug delivery and biomedical applications. *Nanomedicine*. 2015;11(2):313–327. doi:10.1016/j.nano.2014.09.014
12. Chen J, Wei Y, Yang X, Ni S, Hong F, Ni S. Construction of selenium-embedded mesoporous silica with improved antibacterial activity. *Colloids Surf B Biointerfaces*. 2020;190:110910. doi:10.1016/j.colsurfb.2020.110910
13. Nemmar A, Yuvaraju P, Beegam S, Yasin J, Kazzam EE, Ali BH. Oxidative stress, inflammation, and DNA damage in multiple organs of mice acutely exposed to amorphous silica nanoparticles. *Int J Nanomedicine*. 2016;11:919–928. doi:10.2147/IJN.S92278
14. Du ZJ, Cui GQ, Zhang J, et al. Inhibition of gap junction intercellular communication is involved in silica nanoparticles-induced H9c2 cardiomyocytes apoptosis via the mitochondrial pathway. *Int J Nanomedicine*. 2017;12:2179–2188. doi:10.2147/IJN.S127904
15. Chen Z, Meng H, Xing G, et al. Age-related differences in pulmonary and cardiovascular responses to SiO2 nanoparticle inhalation: nanotoxicity has susceptible population. *Environ Sci Technol*. 2008;42(23):8985–8992. doi:10.1021/es800975u
16. Duan J, Yu Y, Li Y, et al. Low-dose exposure of silica nanoparticles induces cardiac dysfunction via neutrophil-mediated inflammation and cardiac contraction in zebrafish embryos. *Nanotoxicology*. 2016;10(5):575–585. doi:10.3109/17435390.2015.1102981
17. Duan J, Yu Y, Li Y, Yu Y, Sun Z. Cardiovascular toxicity evaluation of silica nanoparticles in endothelial cells and zebrafish model. *Biomaterials*. 2013;34(23):5853–5862. doi:10.1016/j.biomaterials.2013.04.032
18. Duan J, Hu H, Feng L, Yang X, Sun Z. Silica nanoparticles inhibit macrophage activity and angiogenesis via VEGFR2-mediated MAPK signaling pathway in zebrafish embryos. *Chemosphere*. 2017;183:483–490. doi:10.1016/j.chemosphere.2017.05.138
19. Guerrero-Beltran CE, Bernal-Ramirez J, Lozano O, et al. Silica nanoparticles induce cardiotoxicity interfering with energetic status and Ca^{2+}++ handling in adult rat cardiomyocytes. *Am J Physiol Heart Circ Physiol*. 2017;312(4):645–661. doi:10.1152/ajpheart.00564.2016
20. Ibarra J, Morley GE, Delmar M. Dynamics of the inward rectifier K^+ current during the action potential of guinea pig ventricular myocytes. *Biophys J*. 1991;60(6):1534–1539. doi:10.1016/S0006-3495(91)82187-7
21. Priest BT, McDermott JS. Cardiac ion channels. *Channels (Austin)*. 2015;9(6):352–359. doi:10.1080/19336950.2015.1076597
22. Lin CX, Yang SY, Gu JL, Meng J, Xu HY, Cao JM. The acute toxic effects of silver nanoparticles on myocardial transmembrane potential, INa and IK1 channels and heart rhythm in mice. *Nanotoxicology*. 2017;11:827–837. doi:10.1080/17435390.2017.1367047
23. Lin CX, Gu JL, Cao JM. The acute toxic effects of platinum nanoparticles on ion channels, transmembrane potentials of cardiomyocytes in vitro and heart rhythm in vivo in mice. *Int J Nanomedicine*. 2019;14:5595–5609. doi:10.2147/IJN.S209135
24. Anumonwo JM, Lopatin AN. Cardiac strong inward rectifier potassium channels. *J Mol Cell Cardiol*. 2010;48(1):45–54. doi:10.1016/j.yjmcc.2009.08.013
25. Carmeliet E. Cardiac ionic currents and acute ischemia: from channels to arrhythmias. *Physiol Rev*. 1999;79:917–1017. doi:10.1152/physrev.1999.79.3.917
26. Wang L, Feng ZP, Kondo CS, Sheldon RS, Duff HJ. Developmental changes in the delayed rectifier K+ channels in mouse heart. *Circ Res*. 1996;79(1):79–85. doi:10.1161/01.res.79.1.79
27. Protas L, Barbuti A, Qu J, et al. Neuropeptide Y is an essential in vivo developmental regulator of cardiac I Ca, L. *Circ Res*. 2003;93(10):972–979. doi:10.1161/01.RES.0000099244.01926.56
28. Lozano O, Silva-Platas C, Chapoy-Villanueva H, et al. Amorphous SiO_2 nanoparticles promote cardiac dysfunction via the opening of the mitochondrial permeability transition pore in rat heart and human cardiomyocytes. *Part Fibre Toxicol*. 2020;17(1):15. doi:10.1186/s12989-020-00346-2
29. Guo C, Xia Y, Niu P, et al. Silica nanoparticles induce oxidative stress, inflammation, and endothelial dysfunction in vitro via activation of the MAPK/Nrf2 pathway and nuclear factor-kappaB signaling. *Int J Nanomedicine*. 2015;10:1463–1477. doi:10.2147/IJN.S76114
30. Liu X, Sun J. Endothelial cells dysfunction induced by silica nanoparticles through oxidative stress via JNK/P53 and NF-kappaB pathways. *Biomaterials*. 2010;31(32):8198–8209. doi:10.1016/j.biomaterials.2010.07.069
31. Zhou F, Liao F, Chen L, Liu Y, Wang W, Feng S. The size-dependent genotoxicity and oxidative stress of silica nanoparticles on endothelial cells. *Environ Sci Pollut Res Int*. 2019;26(2):1911–1920. doi:10.1007/s11356-018-3695-2
32. Handa T, Hirai T, Izumi N, et al. Identifying a size-specific hazard of silica nanoparticles after intravenous administration and its relationship to the other hazards that have negative correlations with the particle size in mice. *Nanotechnology*. 2017;28(13):135101. doi:10.1088/1361-6528/aa5d7c
33. Wang DP, Wang ZJ, Zhao R, et al. Silica nanomaterials induce organ injuries by Ca2+-ROS-initiated disruption of the endothelial barrier and triggering intravascular coagulation. *Part Fibre Toxicol*. 2020;17(1):12. doi:10.1186/s12989-020-00340-8
34. Hinderliter PM, Minard KR, Orr G, et al. ISDD: A computational model of particle sedimentation, diffusion and target cell dosimetry for in vitro toxicity studies. *Part Fibre Toxicol*. 2010;7(1):36. doi:10.1186/1743-8977-7-36